

1   **Evaluating the green potential and optimizing strategies for two**  
2   **industrial brownfields in Harbin, China**

3                   **Cui J<sup>1</sup>, Jia Z-Y<sup>2</sup>, Zhang Y-H<sup>2\*</sup>**

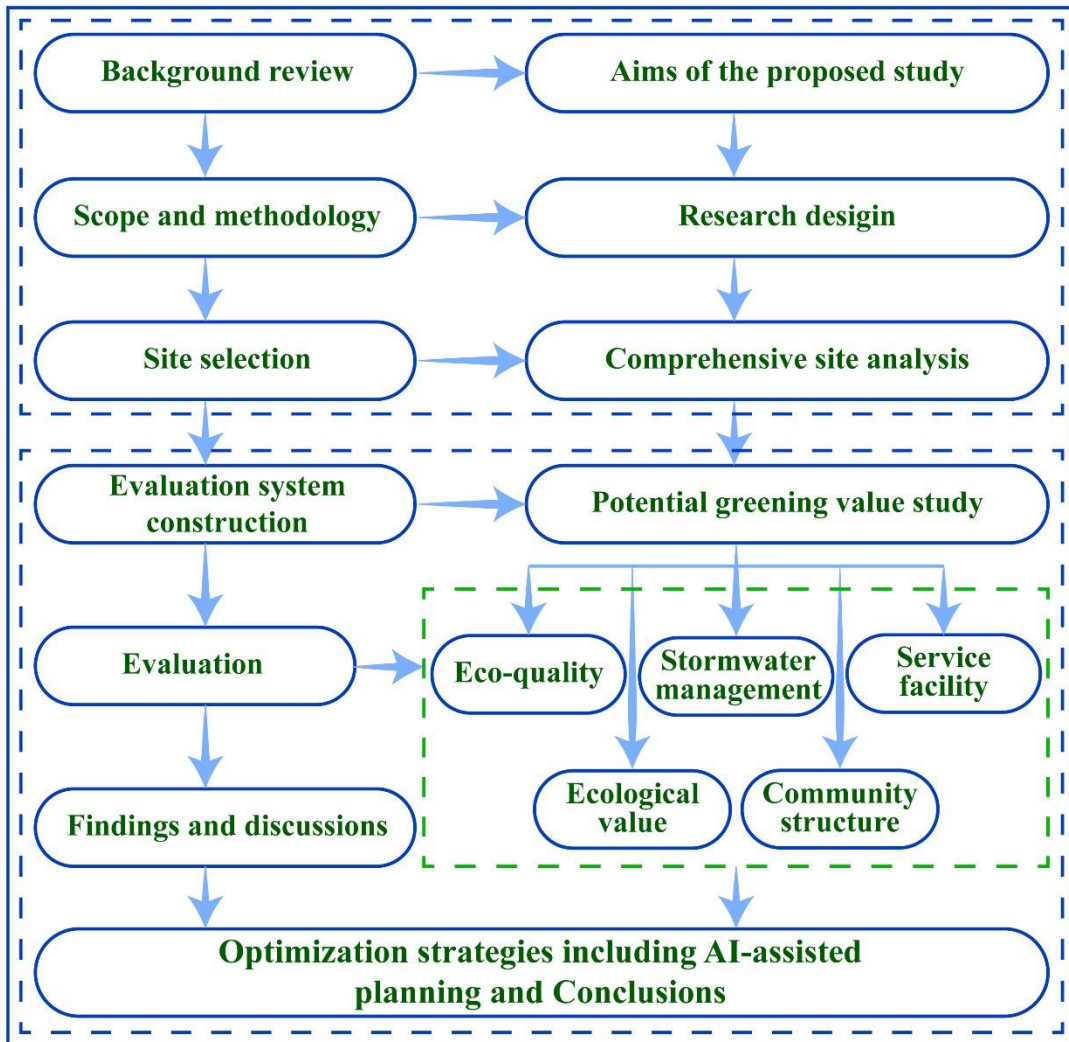
4   1 School of Architecture and Civil Engineering, Faculty of Science, Engineering and  
5   Technology, University of Adelaide, Australia

6   2 M-Grass Ecology And Environment (Group) Co., Ltd, Hohhot, China

7   \*Author to whom correspondence should be addressed [pp7768@126.com](mailto:pp7768@126.com)

8   **Abstract:** With the upgrading of urban industrial structures, the regenerative use of industrial  
9   wasteland has become vital for sustainable urban renewal. Transforming such sites into green  
10   spaces can alleviate urban green space shortages and improve ecological quality. This study  
11   focuses on two distinct industrial wasteland sites in Harbin's Xiangfang District, namely the  
12   former Xingguang Machinery Factory (XMF) and the former Textile Printing and Dyeing  
13   Factory (TPDF). A green value evaluation system comprising five criterion layers and 21  
14   indicators was established using the Analytic Hierarchy Process (AHP), and field surveys and  
15   GIS analysis were applied for assessment. The results indicate that XMF (score 3.76) exhibits  
16   significantly higher green value than TPDF (score 2.44), mainly due to differences in ecological  
17   quality, pollution levels, and urban integration. Differentiated regeneration strategies  
18   incorporating AI-assisted planning (e.g., machine learning for contamination mapping and  
19   generative design for spatial configuration) are proposed. For XMF, an ecology-culture  
20   integrated park is recommended, while for TPDF, an art-led green cultural-creative district with  
21   zoned remediation is suggested. This research offers a scientifically supported and technology-  
22   informed approach for the sustainable regeneration of industrial wasteland.

23   **Keywords:** industrial brownfield, green value evaluation, analytic hierarchy process (AHP);  
24   landscape optimization strategy, Harbin



25

26

Graphical abstract

27 **1. Introduction**

28       Rapid urbanization and the advent of the post-industrial era have led to the emergence of  
 29 numerous industrial wastelands within cities (Accordino & Johnson, 2000). The formation of  
 30 these sites results from the interplay of various complex factors, including global and local  
 31 economic changes, climatic conditions, social structure, political decisions, population  
 32 movements, and cultural context (Cui et al., 2025; Hwang & Lee, 2019; Mrak et al., 2022;  
 33 Newman et al., 2018). During industrial transformation and urban renewal, numerous  
 34 brownfields and abandoned plots have emerged as legacy spaces that cannot be overlooked in  
 35 urban development (Chien & Knoble, 2024; Qu et al., 2020; Song et al., 2020).

36 These areas not only face problems such as soil pollution, ecological degradation, and  
37 landscape fragmentation (Adams et al., 2010), but also fragment the city's physical structure  
38 and visual landscape to some extent, while harboring environmental pollution and public safety  
39 risks that pose potential threats to residents' lives (Beam et al., 2021; Cui et al., 2022; Cundy  
40 et al., 2016). However, from the perspective of urban ecological restoration, these brownfield  
41 resources, often seen as "urban scars", can be transformed into important catalysts for urban  
42 vitality. Their conversion into urban green spaces can bring profound impacts for sustainable  
43 urban development (Anderson & Minor, 2017; Preston et al., 2024; Rupprecht & Byrne, 2014;  
44 Stanford et al., 2025). This transformation is significant for alleviating construction land  
45 shortages, improving residents' quality of life, and preserving industrial culture (Adams et al.,  
46 2010).

47 In recent years, researchers and practitioners worldwide have continuously explored  
48 diverse regeneration strategies including ecological restoration, landscape remodeling, and  
49 functional replacement, while introducing cutting-edge technologies such as artificial  
50 intelligence to enhance the scientific rigor and foresight of industrial wasteland redevelopment  
51 (Mao et al., 2022; Naghibi et al., 2021; Song et al., 2022; Xi, 2024). However, current research  
52 predominantly focuses on overall transformation models or discussions of single cases, while  
53 comparative studies examining the inherent characteristics and differences in greening potential  
54 among different types of industrial wasteland remain insufficient (Derudder & Taylor, 2021;  
55 Fu et al., 2024). Particularly, wastelands originating from different industrial sectors (e.g.,  
56 heavy industry vs. light industry) exhibit essential differences in historical context, spatial  
57 structure, pollution levels, and other aspects, which inevitably lead to differentiation in their  
58 green value and regeneration pathways (Draus et al., 2020; Gobster et al., 2020; Hsiao, 2022).  
59 Current research on evaluation systems and differentiated strategies for urban wasteland  
60 utilization requires further enhancement (Cui et al., 2025). How to scientifically evaluate  
61 greening potential and formulate targeted landscape optimization strategies has become a  
62 research hotspot in fields such as landscape architecture, urban and rural planning, and urban  
63 ecology (Akkerman & Cornfeld, 2009; Atkinson et al., 2014; Cady et al., 2020; Chen &  
64 Hashimoto, 2025).

65 Against the backdrop above, a key scientific question arises: Do brownfields originating  
66 from different industrial sectors exhibit significantly different green potentials, and which  
67 ecological or social factors primarily drive these differences? To address this, it is necessary to

68 move beyond established ecosystem service-based or ecological security pattern models (e.g.,  
69 Cundy et al., 2016; Atkinson et al., 2014). This study aims to develop a novel green value  
70 evaluation system that integrates and weighs sector-specific factors (such as legacy pollution  
71 level, landscape structural adaptability, and cultural-historical value) with multi-dimensional  
72 urban integration indicators. This approach seeks to capture the distinct greening constraints  
73 and opportunities inherent to different industrial histories, thereby offering a more nuanced tool  
74 for comparative potential assessment and differentiated strategy formulation.

75 Harbin, China, as a typical representative of China's old industrial base, has the rise and  
76 fall of industrial civilization deeply imprinted in its urban fabric. Xiangfang District, located in  
77 the southeast of the city, served not only as a pioneering area for industrialization in Northeast  
78 China but also accumulated a large number of different types of industrial heritage and  
79 wasteland during the tides of the era. This study selects two highly contrasting typical cases  
80 within this region. The first is the former Xingguang Machinery Factory (XMF), which was  
81 military-industrial in nature with sturdy and grand buildings and relatively singular pollution.  
82 The second is the former Textile Printing and Dyeing Factory (TPDF), which was involved in  
83 textile printing and dyeing with lighter buildings but complex and severe pollution. This stark  
84 contrast between "hard and soft", "heavy and light" provides an excellent sample for addressing  
85 the research question.

86 Building on the proposed evaluation framework, this paper aims to quantitatively analyze  
87 the differences in greening potential between the two sites. Through site visits, questionnaires,  
88 field investigations, expert evaluations, and the Analytic Hierarchy Process (AHP) method, a  
89 comprehensive assessment of the greening potential of the two sites was conducted. Based on  
90 the evaluation results, this study proposes landscape optimization strategies matching their  
91 respective characteristics, aiming to provide a scientifically supported and differentiated  
92 approach for ecological restoration and landscape regeneration of similar industrial wastelands.

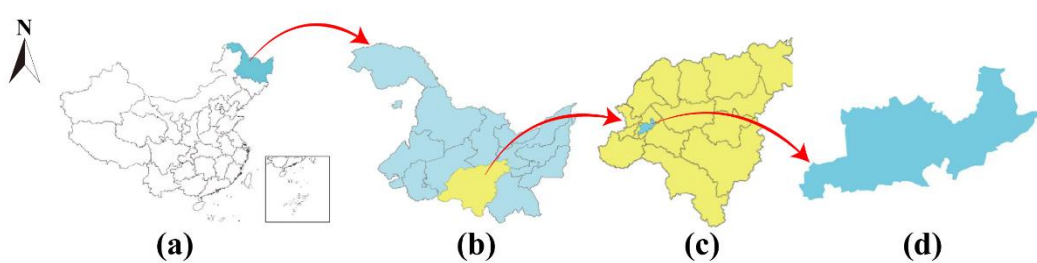
93 **2. Materials and Methods**

94 **2.1 Study Area Overview**

95 Harbin (45°40'- 48°40'N, 125°40'-130°10'E) is located in Northeast China, the capital of  
96 Heilongjiang province, situated in the middle reaches of the Songhua River (You, 2024). The  
97 total area of Harbin is about 53,000 km<sup>2</sup>, making it one of the provincial capitals with the

98 largest area in China (Xu and Xu, 2020). Harbin was once a key industrial base constructed in  
99 the early years of the People's Republic of China. Through the 'Southern Factory Relocation  
100 North' and the layout of several national major projects, it gradually formed an industrial  
101 system supported by large and medium-sized state-owned enterprises and covering  
102 comprehensive categories. Its power station equipment, precision bearings, military products,  
103 etc., were at the forefront of the country in terms of technical capability and industrial scale,  
104 becoming an important force driving national industrialization and regional economic growth  
105 (Zhang et al., 2023). The heavy industrial bases in the early founding period were mainly  
106 located in the Xiangfang District in the southeast of Harbin (Ge, 2017), as shown in Figure 1.

107

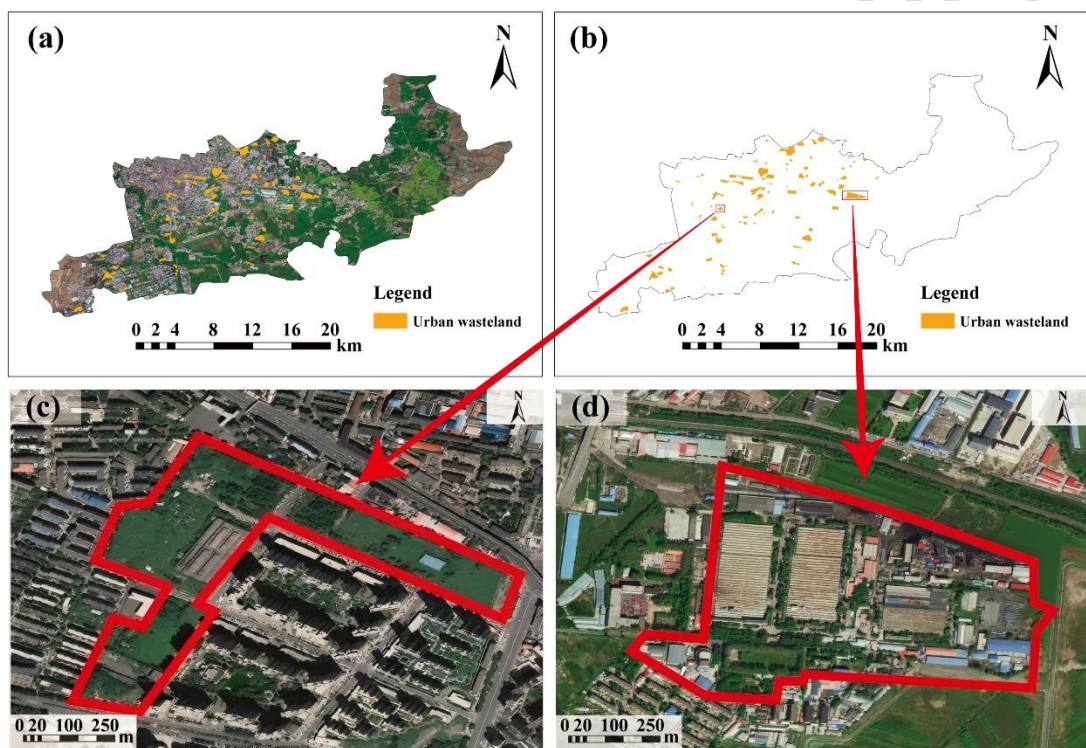


108 **Figure 1.** Location Map of Xiangfang District, Harbin City. (a) Outline Map of China; (b)  
109 Outline Map of Heilongjiang Province; (c) Outline Map of Harbin City; (d) Outline Map of  
110 Xiangfang District.

111 With the advancement of the market economy transition in recent years, the traditional  
112 industrial structure long relied upon by Harbin struggled to adapt to diversified demands, and  
113 many enterprises faced challenges of overcapacity and lagging technological upgrades. Against  
114 the backdrop of urban functional adjustment and industrial relocation, many old factory sites  
115 were successively closed, relocated, or transformed, with the original sites gradually turning  
116 into residential and commercial land. For example, the original Linen Factory, Cement Factory,  
117 and other plots have been developed into new urban functional areas. Simultaneously, some  
118 factory buildings have been preserved and transformed into cultural and creative parks or  
119 commercial spaces, becoming typical cases of industrial heritage reuse. In this process, a  
120 considerable number of old factory areas have been left idle and abandoned for various reasons,  
121 forming a considerable scale of industrial wasteland, such as the concentrated abandoned  
122 factory areas of bearing factories, timber factories, chemical plants, machinery factories, silk  
123 spinning mills, and textile printing and dyeing factories in Xiangfang District. These sites not

124 only affect land value and the urban environment but also reflect the growing pains of regional  
125 industrial structure adjustment.

126 Based on the identification of wasteland in Harbin's Xiangfang District using high-  
127 resolution satellite imagery (Gaofen-6) combined with ArcGIS 10.8, along with preliminary  
128 field surveys assisted by drone technology (DJI Goggles 2), this study selected two distinct  
129 types of industrial wasteland, namely the former military-industrial Xingguang Machinery  
130 Factory (XMF) and the former textile printing and dyeing factory (TPDF), for research on  
131 differences in greening potential (Figure 2).



132

133 **Figure 2.** Geographical Context and Satellite Imagery of the XMF and TPDF Industrial  
134 Wasteland Sites. (a) and (b): Locator maps showing the position of the sites within Xiangfang  
135 District; (c) and (d): High-resolution satellite image overviews of the XMF and TPDF sites,  
136 respectively.

137 XMF was established in 1965, as a military enterprise directly under the former Ministry  
138 of Aerospace Industry. The site area is 21.22 hectares. Some internal factory buildings have  
139 been demolished, but the core protective buildings are relatively intact. The green coverage rate  
140 is high, reaching 84.91%, and vegetation growth is good. Pollution sources are mainly heavy

141 metals and lubricating oil from machining. TPDF was built in the 1980s, as a comprehensive  
142 textile enterprise. The site area is 49.60 hectares. Most of the internal factory structures remain,  
143 but there is a lot of hardened ground. Pollution mainly comes from dyes, auxiliaries, and organic  
144 wastewater from the printing and dyeing process, with complex composition and high treatment  
145 difficulty. The green coverage rate is low, only 32.01%. Aerial photographs of the two  
146 wasteland sites are shown in Figure 3; they were acquired in June 2024.



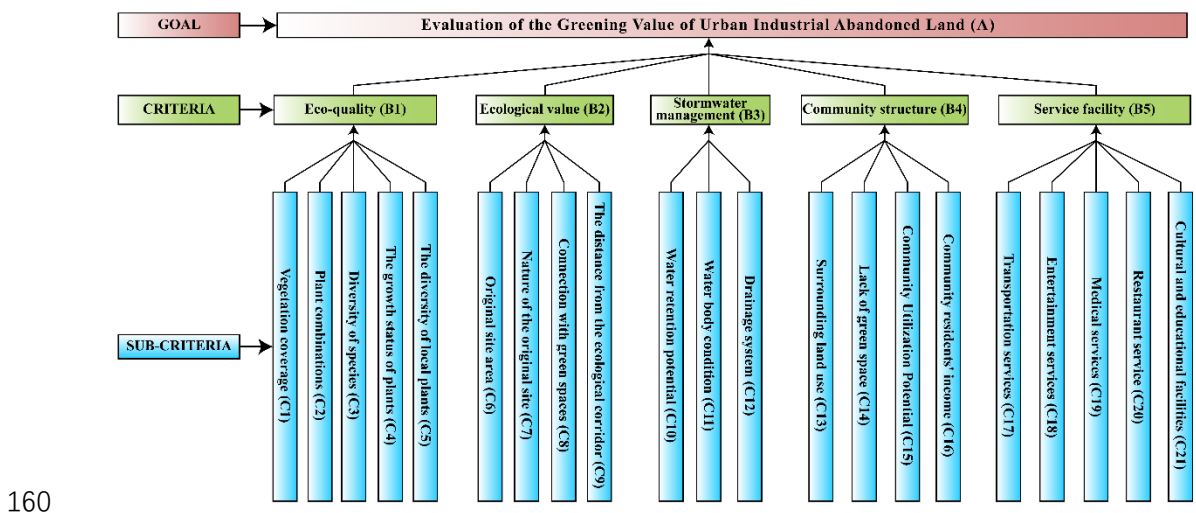
147

148 **Figure 3.** Aerial photographs of the XMF and TPDF industrial wasteland sites. (a1-a4) The  
149 XMF site, shown from different viewing angles; (b1-b4) The TPDF site, shown from different

150 viewing angles. The area enclosed by the red line demarcates the extent of the factory  
151 premises, with the area beyond it defined as the surrounding zone.

152 **2.2 Construction of the Green Value Evaluation System**

153 This study employed the Analytic Hierarchy Process (AHP) to construct the evaluation  
154 system (Byun, 2001). The goal layer (A) is Green Value. The criterion layer (B) consists of five  
155 aspects: Eco-quality (B1), Ecological Value (B2), Stormwater Management (B3), Community  
156 Structure (B4), and Service Facilities (B5). The indicator layer (C) includes 21 specific  
157 indicators, such as Vegetation Coverage (C1), Original Site Area (C6), Water Retention  
158 Potential (C10), Community Utilization Potential (C15), Transportation Services (C17), etc.  
159 The hierarchical structure model of the green value evaluation system is detailed in Figure 4.



160  
161 **Figure 4.** Analytic Hierarchy Process (AHP) model for evaluating the green value of  
162 industrial wasteland.

163 **2.3 Procedure of Consultation and Questionnaire Administration**

164 A panel of experts specializing in landscape architecture, urban planning, and architectural  
165 engineering was assembled (see Supplementary Table 1). Expert selection criteria included:  
166 holding an associate senior professional title or above, having over 10 years of research or  
167 practical experience in related fields, and possessing hands-on project experience in industrial  
168 heritage regeneration or ecological restoration. The expert panel conducted pairwise  
169 comparisons of indicators through a combination of field visits and structured interviews to  
170 construct judgment matrices.

171 A total of 200 questionnaires were distributed to residents surrounding each site, resulting  
172 in 368 valid responses, representing a response rate of 92%. The demographic profile of  
173 respondents was as follows: the majority (62%) were aged 30-50, most (71%) held a college  
174 degree or higher, and occupations included employees of enterprises and institutions, self-  
175 employed individuals, students, and retirees. Respondents rated the importance of the 21  
176 specific indicators using a 5-point Likert scale (1-5).

177 **2.4 Weight Determination and Consistency Check**

178 The geometric mean method was applied to aggregate data from expert judgment matrices  
179 and resident questionnaires to calculate the weights of indicators at each level. All judgment  
180 matrices passed the consistency check, with Consistency Ratio (CR) values as follows: 0.043  
181 (Criterion layer A), 0.028 (Eco-quality B1), 0.036 (Ecological value B2), 0.021 (Stormwater  
182 management B3), 0.039 (Community structure B4), and 0.031 (Service facilities B5).

183 All CR values were below 0.1, satisfying the consistency requirement. Final weights and  
184 rankings are presented in Table 1. The weight analysis revealed that Ecological Value (B2) and  
185 Eco-quality (B1) are the most critical factors determining green value, ranking first and second,  
186 respectively.

187 **Table 1. Weights and ranking of green potential evaluation for each criteria**

A	B1	B2	B3	B4	B5	Wi	Order
B1	1	0.2703	3.8912	3.1436	2.1748	0.2242	2
B2	3.7037	1	4.9206	3.9603	4.0315	0.4597	1
B3	0.2571	0.2033	1	0.2924	0.3618	0.0556	5
B4	0.3185	0.2525	3.4483	1	2.8624	0.1575	3
B5	0.4608	0.2481	2.7778	0.3497	1	0.1030	4

188 *Note: The meanings of each code as shown in Figure 4.*

189 **2.5 Model Validation and Sensitivity Analysis**

190 To assess the robustness of the evaluation model, a sensitivity analysis was conducted.  
191 Weights at the criterion level were randomly varied within a range of  $\pm 10\%$  to observe their  
192 impact on the total green value scores. Results indicated that under these weight fluctuations,  
193 the green value levels of the two study sites remained stable. This demonstrates the model's

194 reliability and the credibility of the evaluation outcomes. Furthermore, the questionnaire survey  
195 results of this study also confirmed the stability of the model.

196 **2.6 Data Sources and Processing**

197 Data sources include the following aspects: (1) High-resolution satellite imagery (Gaofen-  
198 6) from 2022, and aerial imagery (DJI Goggles 2) from 2024; (2) Experts field survey and  
199 vegetation quadrat survey; (3) Relevant urban planning documents and GIS database of  
200 Xiangfang District; (4) Residents questionnaire survey.

201 Scores for each indicator were quantified based on pre-established scoring criteria  
202 (Supplementary Table 2, Table 3, Table 4, Table 5, Table 6). Statistical significance of  
203 differences between groups was determined using the Student's t-test (Barrado et al., 2016),  
204 and associations between variables were assessed by Pearson correlation analysis (Mo et al.,  
205 2025).

206 **2.7 Comprehensive Evaluation Model**

207 The comprehensive index evaluation method was used to calculate the total green value  
208 score (A), with the formula as follows:

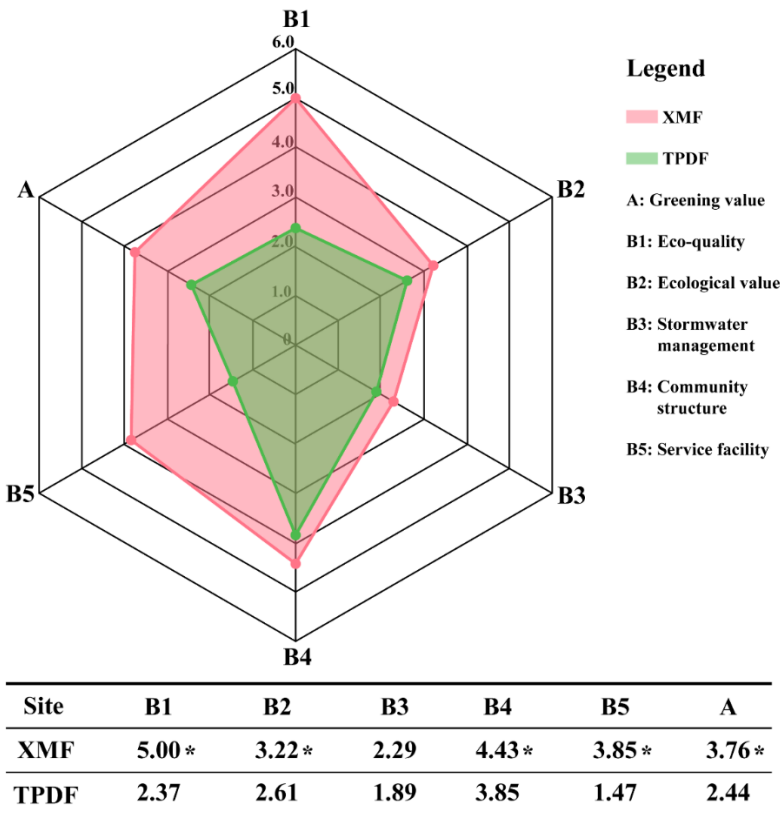
209 
$$A = \Sigma (B_i \times W_i)$$

210 Here,  $B_i$  is the score of the  $i$ -th criterion layer, and  $W_i$  is its corresponding weight. The  
211 criterion layer score  $B_i$  is obtained by the weighted sum of its subordinate indicator layer scores.  
212 Scores are given on a 5-point scale (1, 2, 3, 4, 5). The value is categorized as follows: 'Low'  
213 for scores in the [1-2] range, 'Medium' for [2-3], 'High' for [3-4], and 'Very High' for [4-5].

214 **3. Results and Analysis**

215 **3.1 Comprehensive Green Value Evaluation Results**

216 According to the comprehensive evaluation model calculation, the total green value  
217 scores and various criterion layer scores for the XMF and TPDF sites are shown in Figure 5.



218

219 **Figure 5.** Comparison of Green Value Evaluation Scores between the XMDF and TPDF Sites.

220 \* indicates a significant differences between XMDF and TPDF ( $p < 0.05$ ).

221 The Figure 5 showed that all scores of different criteria layers in XMDF were higher than  
 222 in TPDF. And also the total green value score of the XMDF (3.76) is significantly higher than  
 223 that of the TPDF site (2.44). This indicates that, in terms of comprehensive potential for  
 224 transformation into green space, the Xingguang Machinery Factory is superior to the Textile  
 225 Printing and Dyeing Factory.

226 **3.2 Comparative and Correlative Analysis of Greening Values**

227 To elucidate the underlying causes of the differences in total green value, a detailed  
 228 comparison across the five criterion layers was conducted (Figure 5). The scores and weighted  
 229 contributions of each sub-criterion (C1 - C21) are presented in Table 2.

230 **Table 2. Score and weight of each sub-criteria for calculating greening value (B1 to B5)**

Sub-criteria	Score in XMDF	Score in TPDF	Weight	Sub-criteria	Score in XMDF	Score in TPDF	Weight
C1	5	2	0.0801	C12	1	5	0.0124
C2	5	4	0.0096	C13	5	5	0.0746
C3	5	3	0.0351	C14	3	2	0.0108

C4	5	4	0.0146	C15	5	2	0.0495
C5	5	2	0.0848	C16	2	5	0.0225
C6	4	5	0.1826	C17	4	2	0.0481
C7	2	1	0.1965	C18	4	1	0.0168
C8	5	1	0.0484	C19	4	1	0.0056
C9	3	1	0.0322	C20	4	1	0.0167
C10	3	1	0.0359	C21	3	1	0.0159
C11	1	1	0.0073				

231 The total scores of XMF and TPDF of Eco-quality (B1) in Figure 5 calculated based on  
 232 the comprehensive index evaluation formula that mentioned before, combining with the scores  
 233 in Table 2 and the weights in Supplementary Table 2. The processing are as follows:

234  $XMF=5*0.36+5*0.04+5*0.16+5*0.07+5*0.38=5.00;$

235  $TPDF=2*0.36+4*0.04+3*0.16+4*0.07+2*0.38=2.37.$

236 Also the total scores in Ecological Value (B2), Stormwater Management (B3), Community  
 237 Structure (B4) and Service Facilities (B5) following the same processing above based on Table  
 238 2 and Supplementary Table 3-6.

239 To go beyond the earlier descriptive disparities, a Pearson correlation analysis of the  
 240 combined sites' standardized scores (B1-B5) is conducted here. Results revealed a strong  
 241 positive correlation between Eco-quality (B1) and Stormwater Management (B3) ( $r = 0.89, p <$   
 242 0.01), indicating that sites with better inherent ecological conditions (e.g., higher vegetation  
 243 cover) inherently possess greater potential for stormwater retention that is a synergy evident in  
 244 XMF's superior performance in both aspects. Furthermore, a significant positive correlation  
 245 was found between Community Structure (B4) and Service Facilities (B5) ( $r = 0.92, p < 0.01$ ),  
 246 underscoring that well-integrated urban neighborhoods are typically accompanied by more  
 247 complete service infrastructures, as seen in the XMF context.

248 To move beyond description towards causal explanation, the analysis explicitly links  
 249 indicator scores to the sites' industrial typology. The stark contrast in Eco-quality (B1), where  
 250 XMF (5.00) vastly outperformed TPDF (2.37), is directly attributable to their original industrial  
 251 footprints. XMF, as a machinery factory, had extensive interstitial land which underwent  
 252 natural succession after abandonment, leading to high scores in vegetation coverage (C1) and  
 253 local plant diversity (C5). Conversely, TPDF's textile printing and dyeing operations required

254 large areas of hardened ground for logistics and wastewater treatment, resulting in a legacy of  
255 low vegetation coverage and a compromised ecological baseline.

256 The divergence in Ecological value (B2) is fundamentally driven by pollution intensity.  
257 XMF's operations involved localized contaminants like heavy metals. In contrast, TPDF's use  
258 of complex dyes and organic compounds led to widespread, severe contamination. This  
259 intrinsic difference in pollution burden is a primary constraint on TPDF's ecological recovery  
260 potential. Additionally, XMF's superior 'Connection to green spaces' (C8) score is not  
261 incidental but relates to its historical siting within a planned industrial zone near other facilities  
262 with green buffers, enhancing urban ecological connectivity.

263 The assessment of Stormwater management (B3) further validates the link between  
264 industrial legacy and ecosystem function. The high score in XMF is directly tied to its superior  
265 vegetation coverage (C1), which promotes infiltration, despite both sites having poor  
266 underlying permeability due to industrial compaction.

267 Finally, the chasm in Community structure (B4) and Service facilities (B5) finds its root  
268 in the original locational logic of each industry. XMF, as a key state-owned enterprise, was  
269 integrated into a well-serviced urban district from its inception, leading to high surrounding  
270 population density (C15) and complete services (C17). TPDF, with needs for water access and  
271 effluent disposal, was historically situated on the urban fringe. Subsequent urban growth has  
272 not fully integrated this area, leaving it with lower community density and a critical lack of  
273 services, thereby limiting its immediate social utility and accessibility.

274 However, the above statistical and correlational analyses also have certain limitations.  
275 Although two cases are strategically selected for their contrasting typologies, the small sample  
276 size and locations limit the generalizability of the statistical correlations observed. Future work  
277 should expand the number of sites across multiple cities to strengthen the robustness of the  
278 evaluation framework and the derived inter-indicator relationships.

279 **4. Discussion**

280 **4.1 Underlying Reasons for Differences in Green Value**

281 It should be noted that industrial wastelands in different regional and urban contexts often  
282 possess uniqueness in their historical background, spatial characteristics, and social and cultural

283 significance. Therefore, deeply interpreting their formation context and landscape morphology  
284 not only helps understand their local value but also provides key perspectives and  
285 methodological support for formulating more adaptive and humanistic regeneration strategies  
286 (Beames et al., 2018; Li et al., 2018; Li et al., 2024; Preston et al., 2023). The two case studies  
287 selected show prominent differences in green utilization value.

288 The comprehensive green value score of the XMF site (3.76) was substantially higher than  
289 that of the TPDF site (2.44), indicating a significant disparity in their potential for  
290 transformation into urban green space. This divergence stems directly from their distinct  
291 original industrial attributes, which have profoundly shaped their current ecological conditions,  
292 pollution status, and urban integration, as quantified in the evaluation results across the five  
293 criterion layers.

294 First, the stark contrast in Eco-quality (B1), where XMF (5.00) vastly outperformed TPDF  
295 (2.37), is primarily attributable to their differing industrial footprints and subsequent ecological  
296 disturbance. The XMF site, as a machinery factory, featured large, impervious factory buildings  
297 but also extensive interstitial land. After its abandonment, this land experienced minimal  
298 ongoing disturbance, allowing for natural succession. This is evidenced by its top scores in  
299 Vegetation Coverage (C1) and Native Plant Proportion (C5), resulting in a high ecological  
300 baseline. Conversely, the TPDF site, dedicated to textile printing and dyeing, required vast  
301 areas of hardened ground for logistics and wastewater basins, leaving a legacy of low vegetation  
302 coverage (C1) and a compromised ecological foundation that hinders natural recovery.

303 Second, the divergence in Ecological Value (B2) and pollution status is a direct  
304 consequence of their production nature. XMF's military-industrial operations involved  
305 localized pollution, primarily heavy metals and lubricants (C8), categorizing it as a 'Moderately  
306 Polluting Industry'. In contrast, TPDF's use of complex dyes, auxiliaries, and organic  
307 compounds led to widespread and severe contamination, marking it as a 'Heavily Polluting  
308 Industry' (C8). This fundamental difference is reflected in their pollution control difficulty  
309 scores. Furthermore, XMF's superior performance in 'Connection to Green Spaces' (C7) is not  
310 incidental. Its historical placement within a planned industrial zone, often co-located with other  
311 large facilities possessing green buffers, enhanced its connectivity to the urban ecological  
312 network. TPDF, potentially sited for water access and effluent disposal, ended up in a more  
313 isolated location, weakening its ecological linkages.

314        Third, the assessment of Stormwater Management (B3) further underscores the role of pre-  
315 existing site conditions. XMF's higher score (2.29 vs. 1.89 for TPDF) is directly linked to its  
316 superior vegetation coverage (C1), which promotes infiltration and retention, despite both sites  
317 having generally poor underlying permeability due to historical industrial compaction and  
318 construction.

319        Finally, the chasm in urban integration, captured by the Community Structure (B4) and  
320 Service Facilities (B5) criteria, is rooted in their original locational logic and the subsequent  
321 urban development patterns. The XMF site, as part of a significant state-owned industrial base,  
322 was integrated into a well-serviced urban district from its inception. Over time, the surrounding  
323 area developed into mature residential neighborhoods, explaining its high scores for Population  
324 Density (C15), Transportation Services (C17), and other public amenities. Its transformation  
325 into a park thus serves an immediate and dense population. The TPDF site, typical of industries  
326 with specific logistical or environmental needs, was historically situated on the urban fringe.  
327 The subsequent pattern of urban growth has not fully integrated this area, leaving it with lower  
328 community density and a critical lack of service facilities (B5 score: 3.85 for XMF vs. 1.47 for  
329 TPDF), thereby limiting its immediate social demand value and accessibility.

330        In summary, the quantitative evaluation reveals that the 'hard' military-industrial legacy  
331 of XMF conferred a robust ecological and urban-integration advantage. In contrast, the 'soft'  
332 but chemically intensive legacy of the textile industry left TPDF with a more deeply impaired  
333 ecosystem and a peripheral relationship to the urban fabric, necessitating a fundamentally  
334 different regeneration approach.

335        **4.2 Conceptual Differentiated Landscape Optimization Strategies**

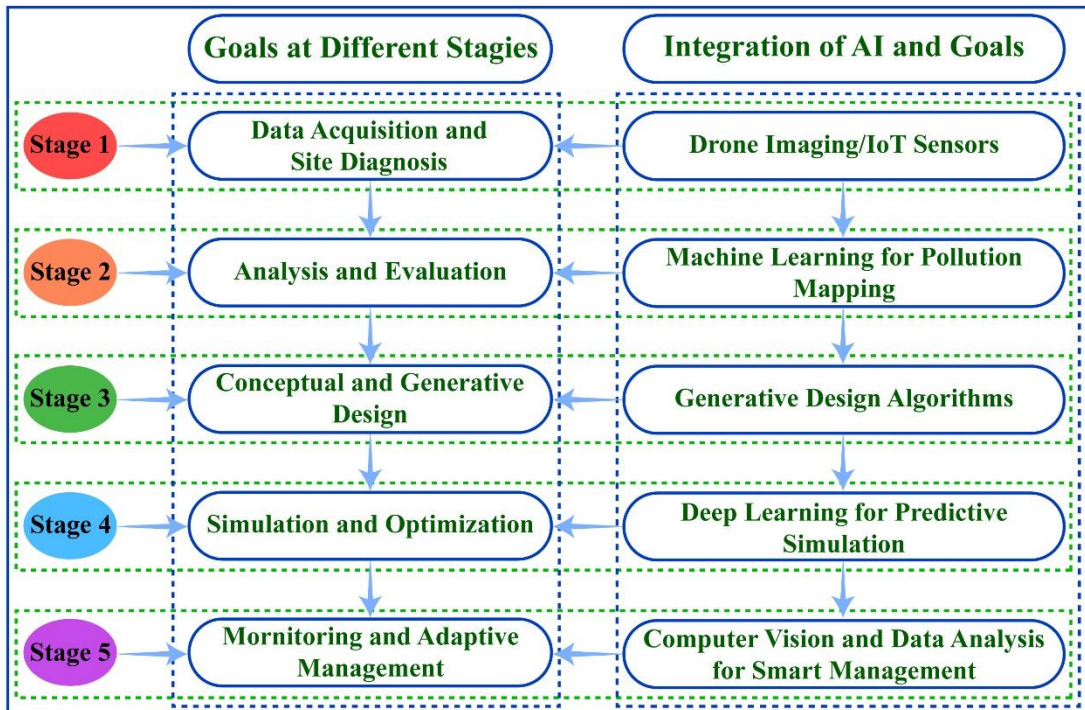
336        Based on the above evaluation and comparison, targeted landscape optimization strategies  
337 are proposed for the two industrial wasteland sites.

338        For XMF site, the strategy proposed an ecology- and culture-integrated comprehensive  
339 park. First, ecological restoration is prioritized by conserving and enhancing existing vegetation  
340 communities to establish a stable near-natural ecosystem. Second, the industrial heritage's  
341 value is revitalized through the adaptive reuse of iconic structure into immersive museums,  
342 exhibition hall, or outdoor art spaces, reinforcing its robust military-industrial cultural character.

343 Third, community needs are met by incorporating facilities for leisure, play, and education,  
344 culminating in an urban park that blends ecology, culture, and recreation.

345 For TPDF site, the strategy focuses on zoned remediation to create an art-led green cultural  
346 district. First, severely polluted printing and dyeing areas undergo risk-based containment,  
347 while less polluted zones receive sensor-guided soil improvement. Second, flexible, low-  
348 intervention approaches are adopted: transforming contaminated zones into land art or hardy  
349 plant displays, and applying 'light-touch' renovations to retained buildings to attract creative  
350 tenants. Third, the site is positioned as a regional fashion art or cultural-creative park with  
351 phased integration into the urban fabric or spur local vitality.

352 To enhance the scientific precision and implementation efficiency of these strategies, an  
353 AI-assisted planning workflow is proposed as shown in Figure 6, integrating specific  
354 technologies into key stages: (1) Site Assessment and Analysis: Machine learning (ML)  
355 algorithms are employed for pollution mapping and predicting ecological restoration potential  
356 by analyzing spatial data such as soil samples and plant vegetation indices. (2) Conceptual and  
357 Generative Design: Using generative design tools (deep learning or optimization algorithms)  
358 to automatically generate and evaluate multiple spatial layout options that meet predefined  
359 constraints (e.g., sun exposure, landscape connectivity, zoning regulations) and objectives such  
360 as preserving heritage structures. (3) Simulation and Optimization: Using deep neural network  
361 simulates long-term outcomes such as vegetation community development, stormwater runoff,  
362 and human foot traffic patterns under different design scenarios. (4) Monitoring and  
363 Management: Using computer vision and internet of things (IoT) sensor networks to monitor  
364 soil health, plant growth, and visitor flows, supporting adaptive management post-construction.



365

366 Figure 6. Schematic diagram of the Ai-assisted workflow for industrial brownfield regeneration  
 367 planning.

368 **5. Conclusion**

369 This study quantitatively evaluated and compared the green value of two typical industrial  
 370 wastelands, XMF and TPDF, in Harbin, China. The main conclusions are as follows:

371 (1) The green value evaluation system developed effectively quantifies the potential of  
 372 industrial wastelands for transformation into urban green spaces. Significant differences in  
 373 ecological baselines, pollution levels, and urban integration resulted in XMF (3.76)  
 374 outperforming TPDF (2.44).

375 (2) Original industrial attributes critically shape all aspects of green value and must be  
 376 considered in formulating differentiated regeneration strategies.

377 (3) The proposed AI-assisted planning workflow, integrating machine learning for  
 378 contamination mapping, generative design for spatial configuration, and predictive modeling  
 379 for ecosystem simulation, can significantly improve the feasibility, adaptability, and scientific  
 380 robustness of such strategies. For XMF, ecological preservation and cultural enhancement are  
 381 prioritized, while TPDF requires risk control, flexible design, and creativity-driven reactivation.

382 This research confirms the value of evidence-based and technology-supported landscape  
383 design in industrial wasteland regeneration. Future studies should incorporate detailed  
384 engineering measures, cost-benefit analysis, and public participation to strengthen strategy  
385 implementation.

386 **Author Contributions:** Conceptualization, J.C. (Jian Cui) and Y.Z. (Yuehua Zhang);  
387 methodology, J.C. (Jian Cui) and Y.Z. (Yuehua Zhang); software, J.C. (Jian Cui) and Z.J.  
388 (Zhenyu Jia); validation, J.C. (Jian Cui) and Y.Z. (Yuehua Zhang); formal analysis, J.C. (Jian  
389 Cui) and Z.J. (Zhenyu Jia); investigation, Z.J. (Zhenyu Jia) and Y.Z. (Yuehua Zhang); data  
390 curation, J.C. (Jian Cui); writing---original draft preparation, J.C. (Jian Cui); writing---review  
391 and editing, Y.Z. (Yuehua Zhang); funding acquisition, Z.J. (Zhenyu Jia) and Y.Z. (Yuehua  
392 Zhang). All authors have read and agreed to the published version of the manuscript.

393 **Data Availability Statement:** The data presented in this study are available on request from  
394 the corresponding author.

395 **Acknowledgments:** This research has been fully supported by M-Grass Eco. and Environ.  
396 Company under the project number 2022RC-High Level-5.

397 **Conflicts of Interest:** The authors declare no conflict of interest.

## 398 **References**

399 Accordino, J. and Johnson, G. T. (2000). Addressing the vacant and abandoned property  
400 problem. *Journal of Urban Affairs*, 22(3), 301-315. Doi:10.1111/0735-2166.00058.

401 Adams, D., De Sousa, C., Tiesdell, S. (2010). Brownfield development: A comparison of North  
402 American and British approaches. *Urban Studies*, 47(1), 75-104.  
403 Doi:10.1177/0042098009346868.

404 Anderson, E. and C., Minor, E. S. (2017). Vacant lots: An underexplored resource for  
405 ecological and social benefits in cities. *Urban Forestry and Urban Greening*, 21, 146-152.  
406 Doi:10.1016/j.ufug.2016.11.015.

407 Akkerman, A., and Cornfeld, A. F. (2009). Greening as an urban design metaphor: Looking for  
408 the city's soul in leftover spaces. *The Structurist*, 49(50), 30-35.

409 Atkinson, G., Doick, K., Burningham, K., France, C. (2014). Brownfield regeneration to  
410 greenspace: Delivery of project objectives for social and environmental gain. *Urban  
411 Forestry & Urban Greening*, 13(3), 586-594. Doi:10.1016/j.ufug.2013.04.002.

412 Barrado, C., Pérez-Batlle, M., Lopez, M., Pastor, E. (2016). Paired T-test analysis to measure  
413 the efficiency impact of a flying RPAS in the non-segregated airspace. *2016 IEEE/AIAA  
414 35th Digital Avionics Systems Conference (DASC), Sacramento, CA, USA*, 1-7. Doi:  
415 10.1109/DASC.2016.7778008.

416 Beam, D. R., Szabo, A., Olson, J., Hoffman, L., Beyer, K. M. M. (2021). Vacant lot to  
417 community garden conversion and crime in Milwaukee: A difference-in-differences  
418 analysis. *Injury Prevention*, 27(5), 403-408. Doi:10.1136/injuryprev-2020-043767.

419 Beames, A., Broekx, S., Schneidewind, U., Landuyt, D., van der Meulen, M., Heijungs, R.,  
420 Seuntjens, P. (2018). Amenity proximity analysis for sustainable brownfield  
421 redevelopment planning. *Landscape and Urban Planning*, 171, 68-79.  
422 Doi:10.1016/j.landurbplan.2017.12.003.

423 Byun, D. H. (2001). The AHP approach for selecting an automobile purchase model.  
424 *Information & Management*, 38 (5), 289-297. Doi: 10.1016/S0378-7206(00)00071-9

425 Cady, T. J., Rahn, D. A. Brunsell, N. A., Lyles, W. (2020). Conversion of abandoned property  
426 to green space as a strategy to mitigate the urban heat island investigated with numerical  
427 simulations. *Journal of Applied Meteorology and Climatology*, 59(11), 1827-1843.  
428 Doi:10.1175/JAMC-D-20-0093.1.

429 Chen, B., Hashimoto, S. (2025). Integrate brownfield greening into urban planning: A review  
430 from the perspective of ecosystem services. *Urban Forestry & Urban Greening*, 104,  
431 128642. Doi:10.1016/j.ufug.2024.128642.

432 Chien, S.-C., Knoble, C. (2024). Uneven burdens: The intersection of brownfields, pollution,  
433 and socioeconomic disparities in New Jersey, USA. *Sustainability*, 16(23), 10535.  
434 Doi:10.3390/su162310535.

435 Cui, J., Jensen, S. T., MacDonald, J. (2022). The effects of vacant lot greening and the impact  
436 of land use and business presence on crime. *Environment and Planning B: Urban*  
437 *Analytics and City Science*, 49(3), 1147-1158. Doi:10.1177/23998083211050647.

438 Cui, J.; Sharifi, E.; Bartesaghi Koc, C.; Yi, L.; Hawken, S. (2025). Factors shaping biodiversity  
439 in urban voids: A systematic literature review. *Land*, 14, 821. Doi: 10.3390/land14040821.

440 Cundy, A. B., Bardos, R. P., Puschenreiter, M., Mench, M., Bert, V., Friesl-Hanl, W., Muller,  
441 I., Li, X. N., Weyens, N., Witters, N., Vangronsveld, J. (2016). Brownfields to green fields:  
442 Realizing wider benefits from practical contaminant phytomanagement strategies. *Journal*  
443 *of Environmental Management*, 184(1), 67-77. Doi:10.1016/j.jenvman.2016.03.028.

444 Derudder, B. and Taylor, P. J. (2021). Not Chicago: Voids in world city network formation.  
445 *Urban Geography*, 42(10), 1500-1524. Doi:10.1080/02723638.2020.1810490.

446 Draus, P., Haase, D., Napieralski, J., Sparks, A., Qureshi, S., Roddy, J. (2020). Wastelands,  
447 greenways and gentrification: Introducing a comparative framework with a focus on  
448 Detroit, USA. *Sustainability*, 12(15), 6189. Doi:10.3390/su12156189.

449 Fu, Q., Han, Y., Xiang, S., Zhu, J., Zhang, L., Zheng, X. (2024). Spatial characteristics of  
450 brownfield clusters and city-brown patterns: Case studies of resource-exhausted cities in  
451 China. *Land*, 13(8), 1251. Doi:10.3390/land13081251.

452 Ge, Y.W. (2017). Suggestions on further promoting the construction of Harbin smart city:  
453 Based on the investigation of the current situation of Xiangfang District smart city  
454 construction. *Decision Consulting*, (3), 16-19. Doi: 10.3969/j.issn.1006-3404.2017.03.007.

455 Gobster, P. H., Hadavi, S., Rigolon, A., Stewart, W. P. (2020). Measuring landscape change,  
456 lot by lot: Greening activity in response to a vacant land reuse program. *Landscape and*  
457 *Urban Planning*, 196, e103729. Doi:10.1016/j.landurbplan.2019.103729.

458 Hsiao, H. (2022). Spatial distribution of urban gardens on vacant land and rooftops: A case  
459 study of 'The Garden City Initiative' in Taipei City, Taiwan. *Urban Geography*, 43(8),  
460 1150-1175. Doi:10.1080/02723638.2021.1901036.

461 Hwang, S.W. and Lee, S.J. (2019). Unused, underused, and misused: An examination of  
462 theories on urban void spaces. *Urban Res. Pract.* 13(5), 540-556.  
463 Doi:10.1080/17535069.2019.1634140.

464 Li, M., Li, R., Liu, X., Fabris, L. M. F. (2024). A brownfield regeneration in urban renewal  
465 contexts visual analysis: research hotspots, trends, and global challenges. *Landscape*  
466 *Research*, 49(6), 896-911. Doi:10.1080/01426397.2024.2359521.

467 Li, Y., Chen, X., Tang, B., Wong, S. (2018). From project to policy: Adaptive reuse and urban  
468 industrial land restructuring in Guangzhou city, China. *Cities*, 82, 68-76.  
469 Doi:10.1016/j.cities.2018.05.006.

470 Mao, L., Zheng, Z., Meng, X., Zhou, Y., Zhao, P., Yang, Z., Long, Y. (2022). Large-scale  
471 automatic identification of urban vacant land using semantic segmentation of high-  
472 resolution remote sensing images. *Landscape and Urban Planning*, 222, e104384.  
473 Doi:10.1016/j.landurbplan.2022.104384.

474 Mo, J.T., Liu, F., Deng, X.X. (2025). A group decision making model with non-reciprocal fuzzy  
475 preference relations based on Pearson correlation coefficient. *Expert Systems with*  
476 *Applications*, 276. Doi:10.1016/j.eswa.2025.127095.

477 Mrak, I., Ambrušs, D., Marović, I. (2022). A holistic approach to strategic sustainable  
478 development of urban voids as historic urban landscapes from the perspective of urban  
479 resilience. *Buildings*, 12(11), 1852. Doi:10.3390/buildings12111852.

480 Naghibi, M., Faizi, M., Ekhlassi, A. (2021). Design possibilities of leftover spaces as a pocket  
481 park in relation to planting enclosure. *Urban Forestry & Urban Greening*, 64, e127273.  
482 Doi:10.1016/j.ufug.2021.127273.

483 Newman, G., Park, Y., Bowman, A. O. M., Lee, R. J. (2018). Vacant urban areas: Causes and  
484 interconnected factors. *Cities*, 72(B), 421-429. Doi:10.1016/j.cities.2017.10.005.

485 Preston, P. D., Dunk, R. M., Smith, G. R., Cavan, G. (2023). Not all brownfields are equal: A  
486 typological assessment reveals hidden green space in the city. *Landscape and Urban*  
487 *Planning*, 229, e104590. Doi:10.1016/j.landurbplan.2022.104590.

488 Preston, P. D., Dunk, R. M., Smith, G. R., Cavan, G. (2024). Examining regulating ecosystem  
489 service provision by brownfield and park typologies and their urban distribution. *Urban*  
490 *Forestry & Urban Greening*, 95, 128311. Doi:10.1016/j.ufug.2024.128311.

491 Qu, Y., Jiang, G., Li, Z., Shang, R., Zhou, D. (2020). Understanding the multidimensional  
492 morphological characteristics of urban idle land: Stage, subject, and spatial heterogeneity.  
493 *Cities*, 97, e102492. Doi:10.1016/j.cities.2019.102492.

494 Rupprecht, C. D. D. and Byrne, J. A. (2014). Informal urban greenspace: A typology and  
495 trilingual systematic review of its role for urban residents and trends in the literature.  
496 *Urban Forestry & Urban Greening*, 13(4), 597-611. Doi:10.1016/j.ufug.2014.09.002.

497 Song, Y., Lyu, Y., Qian, S., Zhang, X., Lin, H., Wang, S., (2022). Identifying urban candidate  
498 brownfield sites using multi-source data: the case of Changchun City, China. *Land Use*  
499 *Policy*, 117. Doi:10.1016/j.landusepol.2022.106084.

500 Song, X., Wen, M., Shen, Y., Feng, Q., Xiang, J., Zhang, W., Zhao, G., Wu, Z. (2020). Urban  
501 vacant land in growing urbanization: An international review. *Journal of Geographical*  
502 *Sciences*, 30(4), 669-687. Doi:10.1007/s11442-020-1749-0.

503 Stanford, H. R., Hurley, J., Garrard, G. E., Kirk, H. (2025). The contribution of informal green  
504 space to urban biodiversity: a city-scale assessment using crowdsourced survey data.  
505 *Urban Ecosystems*, 28(1), 1-16. Doi:10.1007/s11252-024-01623-0.

506 Xi, S. (2024). Transforming urban industrial wastelands using a CNN-based land classification  
507 model. *Soft Computing*, 28(2), 903-916. Doi:10.1007/s00500-023-09458-1.

508 Xu, A.J. and Xu, D.W. (2020). Research on landscape interactivity based on environmental: A  
509 case study of Lilac Park in Harbin Qunli New Area. *Modern Horticulture*, 43(9), 184-186.  
510 Doi: CNKI:SUN:JXYA.0.2020-09-093

511 You, H.J. (2024). Research on high quality development strategies for Harbin's ice and snow  
512 industry---Against the background of the Harbin Asian Winter Games. *Northern Economy*  
513 *and Trade*, (1), 1-4.

514 Zhang, B.C., Wang, Q.L., Zhang, H. (2023). Research on the survey and protection strategies  
 515 of modern railway architectural heritage in Harbin. *Journal of Suzhou University of*  
 516 *Science and Technology*, 36(4), 39-43.. Doi:10.3969/j.issn.1672-0679.2023.04.006.

517

518 **Supplementary Tables (Note: The meanings of each criteria code in the following tables as**  
 519 **shown in Figure 4.)**

520

521 **Suppl Table 1. Summary of expert consultancy panel composition**

Professional title	Affiliation	Specialty	Participant count	Inquiry method
Professor	Northeast Agricultural University	Landscape architecture	3	Field visit and investigation
Professor	Northeast Forestry University	Landscape architecture	3	Field visit and investigation
Professor	Harbin Institute of Technology	Landscape architecture	2	Field visit and investigation
Professor	Heilongjiang Agricultural Vocational Engineering College	Architectural engineering	2	Field visit and investigation
Associate professor	Heilongjiang Vocational & Technical University of Agricultural Engineering	Landscape architecture	1	Field visit and investigation
Associate professor	Heilongjiang College of Architectural Technology	Urban Architecture	2	Field visit and investigation
Urban designer	Heilongjiang Building Design Institute	Landscape architecture	1	Field visit and investigation
Manager	Harbin Sanfeng Landscape Co., Ltd	Landscape architecture	1	Field visit and investigation

522

523

524 **Suppl Table 2. Weight and ranking of sub-criteria in the eco-quality (B1) dimension**

Sub-criteria	C1	C2	C3	C4	C5	Wi	Order
C1	1	7.0613	3.8602	5.9636	0.8624	0.3573	2
C2	0.1416	1	0.2142	0.3618	0.1836	0.0429	5
C3	0.2591	4.7619	1	4.7141	0.2604	0.1563	3
C4	0.1678	2.7778	0.2123	1	0.1421	0.0651	4
C5	1.1628	5.5556	3.8462	7.1429	1	0.3784	1

525

526 **Suppl Table 3. Weight and ranking of sub-criteria in the ecological value (B2) dimension**

Sub-criteria	C6	C7	C8	C9	Wi	Order
C6	1	1.0624	4.9136	4.3478	0.3973	2
C7	0.9434	1	5.8747	5.5556	0.4274	1
C8	0.2037	0.1704	1	2.4391	0.1053	3
C9	0.2312	0.18	0.41	1	0.0700	4

527

528

529 **Suppl Table 4. Weight and ranking of sub-criteria in stormwater management (B3)**  
530 **dimensions**

Sub-criteria	C10	C11	C12	Wi	Order
C10	1	4.8208	2.9614	0.6456	1
C11	0.2075	1	0.5733	0.1307	3
C12	0.3378	1.7544	1	0.2237	2

531

532

533 **Suppl Table 5. Weights and ranking of sub-criteria in the community structure (B4)**  
534 **dimension**

Sub-criteria	C13	C14	C15	C16	Wi	Order
C13	1	6.8124	1.7802	2.9342	0.4739	1
C14	0.1468	1	0.2641	0.4186	0.0688	4
C15	0.5618	3.8462	1	3.0616	0.3144	2
C16	0.3413	2.439	0.3268	1	0.1429	3

535

536 **Suppl Table 6. Weights and ranking of sub-criteria in the service facilities (B5) dimension**

Sub-criteria	C17	C18	C19	C20	C21	Wi	Order
C17	1	5.0283	4.9321	3.8849	2.7654	0.4667	1
C18	0.1992	1	3.0633	1.8911	1.1228	0.1631	2
C19	0.2028	0.3268	1	0.2942	0.2214	0.0541	5
C20	0.2577	0.5291	3.4483	1	1.9862	0.1621	3
C21	0.3623	0.8929	4.5455	0.5051	1	0.1539	4

537

538

539